Role of polarization mode dispersion on modulational instability in optical fibers

J. Garnier*
Centre de Mathématiques Appliquées, Ecole Polytechnique, 91128 Palaiseau Cedex, France

F. Kh. Abdullaev
Physical-Technical Institute of the Uzbek Academy of Sciences, G. Mavlyanov Street 2-b, 700084 Tashkent, Uzbekistan

E. Seve†
Laboratoire de Physique, Université de Bourgogne, 9 avenue A. Savary, 21011 Dijon, France

S. Wabnitz
Undersea Transmissions Group, Alcatel-CRC, Route de Nozay, 91460 Marcoussis, France
(Received 2 July 2000; revised manuscript received 20 November 2000; published 29 May 2001)

We introduce the theory of modulational instability (MI) of electromagnetic waves in fibers with random polarization mode dispersion. Applying a linear stability analysis and stochastic calculus, we show that the MI gain spectrum reads as the maximal eigenvalue of a constant effective matrix. In the limiting cases of small or large fluctuations, we give explicit expressions for the MI gain spectra. In the general configurations, we give the explicit form of the effective matrix and numerically compute the maximal eigenvalue. In the anomalous dispersion regime, polarization dispersion widens the unstable bandwidth. Depending on the type of variations of the birefringence parameters, polarization dispersion reduces or enhances the MI gain peak. In the normal dispersion regime, random effects may extend the instability domain to the whole spectrum of modulations. The linear stability analysis is confirmed by numerical simulation of the full stochastic coupled nonlinear Schrödinger equations.

DOI: 10.1103/PhysRevE.63.066616 PACS number(s): 42.65.−k, 42.50.Ar, 42.81.Dp

I. INTRODUCTION

Modulational instability (MI) is one of the fundamental processes in nonlinear waves theory [1–5]. Recently, much attention was devoted to MI in inhomogeneous media, particularly periodically varying media [6–8]. MI of electromagnetic waves in random media is the natural extension. Random media encompass all frequencies, so we can expect stochastic resonance phenomena, which are discussed intensively herein. The scalar problem of fluctuating nonlinearity and fluctuating group velocity dispersion (GVD) in fibers has already been studied in Ref. [9] and Refs. [10,11], respectively.

It is interesting to ponder the existence of an analogous phenomenon for the nonlinear evolution of polarization in a birefringent nonlinear dispersive medium with random parameters. An important example is the evolution of the polarization of a continuum wave in a randomly birefringent fiber. Polarization MI was investigated in the deterministic case in Refs. [12,13]. These earlier works discussed the dependence of the gain on the deterministic values of the group-velocity mismatch between polarizations, the frequencies of initial modulations, and the powers of the waves. However, in real fibers, birefringence is not constant, rather it is subject to random fluctuations along the propagation distance [14].

Here we examine the polarization MI of continuum waves in a birefringent fiber with random birefringence. The model for the random birefringent fiber that we consider in this paper is that of polarization-mode dispersion (PMD), which is a random function of propagation distance. PMD is described by a system of two coupled nonlinear Schrödinger (NLS) equations [15]. A model in which the fast and slow axes interchange randomly at given intervals was introduced in Ref. [16]. This model is interesting in that it is the first one to address the problem of random PMD, but it is in some sense incomplete since no power can be scattered between the two polarization modes. In Refs. [17,18], a more sophisticated model was proposed in which the birefringence axes orientation and the phase shift between the modes are randomly varied along the distance. As a consequence, in a fixed reference frame the polarization state of light rotates randomly on the Poincaré sphere. The aim was to investigate soliton stability and radiation under random perturbations. The general model that we deal with in this paper takes into account a group-velocity mismatch between the two polarizations as well as coupling terms between the two polarization modes, which are random functions of propagation distance [19,20].

Note that in this work, we shall neglect fiber loss and competing nonlinear effects, such as stimulated Brillouin scattering, which may be relevant in the propagation of a quasicontinuous wave (cw). As far as loss is concerned, it is well known that in the presence of periodic all-optical amplification, the loss may be averaged out of the propagation whenever the amplifier spacing is small when compared to the characteristic dispersion distance (guiding-center soliton

*Email address: Josselin.Garnier@polytechnique.fr; FAX: (+33).1.69.33.30.11.
†Present address: Alcatel Corporate Research Center, Route de Nozay, 91461, Marcoussis, France.

 ©2001 The American Physical Society

regime of the nonlinear propagation in the fiber). Moreover, Brillouin scattering may be neglected in the presence of relatively wideband signals (still to be considered quasi-cw when compared, for example, with THz modulations) consisting of pump pulses of several picoseconds.

The paper is organized as follows. In Sec. II, the model is formulated. An analysis of the deterministic system is performed in Sec. III. Equations for the mean fields and mean intensities are analyzed in Secs. IV and V. Results of numerical simulations for the full stochastic NLS equations are finally presented in Sec. VI.

II. DESCRIPTION OF THE MODEL

The evolution of polarized fields in randomly birefringent fibers is governed by the coupled nonlinear Schrödinger equations with random PMD between two modes (polarizations) [19,20]:

$$i\vec{A}_z + K\vec{A} + i\Delta\vec{A}_t + \beta\vec{A}_{tt} + \frac{9}{8}\vec{N_1} = \vec{0}, \tag{1}$$

where $\vec{A}$ is the row vector $(A_1,A_2)^T$ that denotes the envelopes of the electric field in the two eigenmodes; we use standard dimensionless variables. The matrices K and Δ describe random fiber birefringence. The GVD coefficient is β, which is positive (negative) for anomalous (normal) dispersion. The $\vec{N_1}$ term stands for the nonlinear terms,

$$\vec{N_1} = \begin{pmatrix} (|A_1|^2 + \alpha|A_2|^2)A_1 + \frac{\alpha}{2}A_2^2A_1^* \\ (|A_2|^2 + \alpha|A_1|^2)A_2 + \frac{\alpha}{2}A_1^2A_2^* \end{pmatrix}, \tag{2}$$

where the cross-phase modulation is $\alpha = \frac{2}{3}$ for linearly birefringent fiber.

As shown by Way and Menyuk, one can eliminate the fast random birefringence variations that appear in Eq. (1) by means of a change of variables, which leads to the new vector equation

$$i\vec{U}_z + i\Omega\vec{U}_t + \beta\vec{U}_{tt} + \vec{N}_2 = \vec{0}, \tag{3}$$

where $\vec{U} \equiv M^{-1}\vec{A}$, $\vec{U} = (u,v)^T$ represents the slow evolution of the field envelopes in the reference frame of the local polarization eigenmodes, and the matrix M obeys the equation $iM_z + KM = 0$. The nonlinear term $\vec{N}_2$ reads

$$\vec{N}_2 = \begin{pmatrix} (|u|^2 + \alpha|v|^2)u \\ (\alpha|u|^2 + |v|^2)v \end{pmatrix}, \tag{4}$$

where the cross-phase modulation $\alpha = 1$ after averaging over fiber birefringence [21].

Ω is a z-dependent matrix that is associated with the coupling between the modes due to perturbations. We consider a general form for Ω:

$$\Omega = S_1\Sigma_1 + S_2\Sigma_2 + S_3\Sigma_3, \tag{5}$$

where Σ_j are Pauli matrices:

$$\Sigma_1 = \begin{pmatrix} 0 & 1 \\ 1 & 0 \end{pmatrix}, \quad \Sigma_2 = \begin{pmatrix} 0 & -i \\ i & 0 \end{pmatrix}, \quad \Sigma_3 = \begin{pmatrix} 1 & 0 \\ 0 & -1 \end{pmatrix},$$

and S_j are real-valued random functions of z. If the fiber is isotropic and if it has a perfectly circularly symmetric cross section, then the S_j are identically zero. If the fiber is birefringent, then S_3 is equal to some constant parameter Δ_0 which may not be zero. Δ_0 is proportional to the group velocity mismatch (GVM) between the two polarization modes. In real units, the GVM reads $\Delta_0 = t_0(k_x' - k_y')/|\beta_2|$, where the primes denote derivatives with respect to ω. However, in real fibers the circular symmetry is broken due to unavoidable imperfections of the fiber. Thus the coefficients S_j acquire z-dependent values. Accordingly, S_1 and S_2 are taken as white Gaussian-distributed noises:

$$\langle S_j(z)\rangle = 0, \quad j = 1,2, \tag{6}$$

$$\langle S_j(z)S_j(z')\rangle = 2\sigma_j^2\delta(z-z'), \quad j = 1,2, \tag{7}$$

while S_3 is taken as the sum of the constant term Δ_0 and a white Gaussian-distributed noise:

$$\langle S_3(z)\rangle = \Delta_0, \tag{8}$$

$$\langle [S_3(z) - \Delta_0][S_3(z') - \Delta_0]\rangle = 2\sigma_3^2\delta(z-z'). \tag{9}$$

In the following, σ_j will be referred to as the standard deviations of the fluctuations of S_j. A simplified model for random birefringence is a random concatenation of different fiber sections whose S_3's have equal absolute values but opposite signs [16]; see also [22]. The lengths of these segments are of the order of $10-100$ m, typically much less than the dispersion distance $L_d = t_0^2/|\beta_2|$. Such configuration may be described by the previous white-noise model with $\sigma_3^2 = [t_0(k_x' - k_y')/|\beta_2|]^2 l_c$, where l_c is the correlation length.

More generally, the presence of the term $\Omega\vec{U}_t$ is associated with linear coupling between the modes, as well as an accumulation of a mismatch between their phases. In spite of this extension, which includes linear mode coupling, the model remains analytically solvable and it predicts some general new features associated with the random nature polarization MI. We believe that these features will be preserved to a large extent in the full numerical simulations of nonlinear pulse propagation in a random fiber, and ultimately in the experiments. For example, an analysis of the stochastic decay of the vector soliton under random variations of S_3 that was performed in the framework of the system (3) [23] leads to practically the same results as the conclusions of a study performed with the *full* model in [19,20]. Note also that the system (3) with $S_1 = S_2 = 0$ was employed for the investigation of resonant phenomena in the solitons dynamics for the case of periodically varying birefringence [24]. In [25], the system (3) with the white-noise model for PMD excitation S_j has been applied to obtain an analytical expression for the jitter due to the interaction with the continuum component. Analogies with the noise-driven harmonic oscil-

lator were observed and confirmed by the numerical simulations of Eq. (3) with white-noise perturbations. We may also remark that whenever $S_j \equiv 0$ and $\alpha = 1$, one obtains the integrable Manakov system.

The nonlinear plane-wave solutions of the system (3) read

$$u_0(z) = A \exp[i(A^2 + \alpha B^2)z], \tag{10}$$

$$v_0(z) = B \exp[i(\alpha A^2 + B^2)z]. \tag{11}$$

Linear stability is evaluated by substituting

$$u(z,t) = [A + u_1(z,t)]\exp[i(A^2 + \alpha B^2)z], \tag{12}$$

$$v(z,t) = [B + v_1(z,t)]\exp[i(B^2 + \alpha A^2)z]. \tag{13}$$

into Eq. (3). By retaining only the first-order terms, one obtains a linear system of equations for u_1 and v_1:

$$iu_{1z} + iS_1 v_{1t} + S_2 v_{1t} + iS_3 u_{1t} + \beta u_{1tt} + 2A^2 \operatorname{Re}(u_1) + 2\alpha AB \operatorname{Re}(v_1) = 0, \tag{14}$$

$$iv_{1z} + iS_1 u_{1t} - S_2 u_{1t} - iS_3 v_{1t} + \beta v_{1tt} + 2B^2 \operatorname{Re}(v_1) + 2\alpha AB \operatorname{Re}(u_1) = 0. \tag{15}$$

In the homogeneous configuration ($S_1 = S_2 \equiv 0$ and $S_3 \equiv \Delta_0$), the MI problem is reduced to an analysis of the eigenvalues of a 4×4 matrix. One can then derive the well-known MI gain spectra of vector modulational instability [26,27]. The main features of this homogeneous configuration will be sketched out in the next section.

If S_j are z-dependent, then a convenient representation of the polarization evolutions induced by the fluctuations S_j may be done in terms of the Stokes vector $\vec{\mathbf{s}}$ associated to the Fourier components of the modulation (u_1, v_1):

$$s_1(\omega) = (|\hat{u}_1|^2 - |\hat{v}_1|^2)(\omega),$$

$$s_2(\omega) = 2 \operatorname{Re}(\hat{u}_1 \hat{v}_1^*)(\omega),$$

$$s_3(\omega) = 2 \operatorname{Im}(\hat{u}_1 \hat{v}_1^*)(\omega),$$

whose modulus $\sqrt{s_1^2 + s_2^2 + s_3^2} = |\hat{u}_1|^2 + |\hat{v}_1|^2$ is proportional to the power at frequency ω. In terms of the Stokes parameters, the dynamics induced by the fluctuations S_j is simple when neglecting the terms arising from the nonlinearity [containing A and B in Eqs. (14) and (15)]:

$$\frac{d\vec{\mathbf{s}}}{dz} = -2\omega \vec{\Theta}(z) \times \vec{\mathbf{s}},$$

where $\vec{\Theta}(z)$ is the row vector $(-S_3, -S_1, S_2)^T(z)$. Thus the S_j appear as elementary infinitesimal generators of random rotations of the Stokes vector over the Poincaré sphere. On the other hand, if we take into account only the nonlinear terms of Eqs. (14) and (15), then we exhibit a coupling between the components of the modulations at frequency ω and $-\omega$. The relevant phenomena thus involve an interplay of the random rotations generated by $\vec{\Theta}$ and the dynamics involved in the nonlinear homogeneous terms. To perform a precise analysis of the system (14) and (15) we use the complex representation $u_1 = C + iD$, $v_1 = E + iF$ and perform the Fourier transform

$$c = \int C e^{i\omega t} dt, \quad d = \int D e^{i\omega t} dt, \tag{16}$$

so that we get the following system for Fourier components:

$$c_z = -i\omega S_1 e - i\omega S_2 f - i\omega S_3 c - \beta\omega^2 d, \tag{17}$$

$$e_z = -i\omega S_1 c + i\omega S_2 d + i\omega S_3 e - \beta\omega^2 f, \tag{18}$$

$$d_z = -i\omega S_1 f + i\omega S_2 e - i\omega S_3 d + \beta\omega^2 c - 2A(Ac + \alpha Be), \tag{19}$$

$$f_z = -i\omega S_1 d - i\omega S_2 c + \omega S_3 f + \beta\omega^2 e - 2B(Be + \alpha Ac). \tag{20}$$

III. DETERMINISTIC SYSTEM

We remind the reader of the results corresponding to the homogeneous configuration $\sigma_j = 0$ [26,27]. In such a case, we have $S_j \equiv 0$, $j = 1,2$, while $S_3 \equiv \Delta_0$. The system of equations for the row vector $\vec{q} := (c,d,e,f)^T$ is

$$\frac{d\vec{q}}{dz} = Q\vec{q}, \tag{21}$$

where Q is the 4×4 matrix,

$$Q = \begin{pmatrix} -i\omega\Delta_0 & \beta\omega^2 & 0 & 0 \\ 2A^2 - \beta\omega^2 & -i\omega\Delta_0 & 2\alpha AB & 0 \\ 0 & 0 & i\omega\Delta_0 & \beta\omega^2 \\ 2\alpha AB & 0 & 2B^2 - \beta\omega^2 & i\omega\Delta_0 \end{pmatrix}. \tag{22}$$

The MI gain is defined as twice the maximal value of the real parts of the eigenvalues of the matrix Q. When it is positive, it governs the exponential growth of the modulation $|\hat{u}_1|^2(\omega) + |\hat{v}_1|^2(\omega)$. The algebra is simplified by considering the case $B = A$. Nevertheless, it should be underlined that this simplification does not affect the generality of the following results and conclusions. We introduce the characteristic frequencies ω_c, ω_-, ω_+, and ω_e:

$$\omega_c := \sqrt{2\beta^{-1}(1+\alpha)A^2},$$

$$\omega_\pm := \sqrt{2\beta^{-1}(1\pm\alpha)A^2 + \beta^{-2}\Delta_0^2},$$

$$\omega_e := \sqrt{2A^2\beta^{-1} - \alpha^2 A^4 \Delta_0^{-2}}.$$

These frequencies may be imaginary. If $\beta > 0$ and $\Delta_0^2 < \alpha^2 \beta A^2/2$, or if $\beta < 0$, then $\omega_e^2 < 0$.

A. Anomalous dispersion $\beta>0$, $\sigma_j=0$

If $\Delta_0=0$, then the frequencies below ω_c are unstable and the corresponding MI gain is

$$G(\omega)=2\beta|\omega|\sqrt{\omega_c^2-\omega^2}. \tag{23}$$

If $\Delta_0\neq 0$ and is such that $\Delta_0^2\leqslant\beta\alpha^2A^2/2$, then there is MI if $|\omega|\leqslant\omega_+$, and the MI gain is

$$G(\omega)=2\beta|\omega|\sqrt{2\beta^{-1}A^2-\beta^{-2}\Delta_0^2-\omega^2+J_0(\omega)}, \tag{24}$$

$$J_0(\omega)=2\beta^{-1}|\Delta_0|\sqrt{\omega^2-\omega_e^2}. \tag{25}$$

If $\Delta_0\neq 0$ and is such that $\beta\alpha A^2>\Delta_0^2>\beta\alpha^2A^2/2$, then there is MI for $|\omega|\leqslant\omega_+$. Note that $0<\omega_e<\omega_-<\omega_+$ since $\omega_\pm^2-\omega_e^2=(\alpha A^2\Delta_0^{-1}\pm\beta^{-1}\Delta_0)^2$. The exact expression of the MI gain can be written on the interval $|\omega|\leqslant\omega_e$ as

$$G(\omega)=\sqrt{2}\beta|\omega|\sqrt{2\beta^{-1}A^2-\beta^{-2}\Delta_0^2-\omega^2+J_1(\omega)}, \tag{26}$$

$$J_1(\omega)=\sqrt{(\omega^2-2\beta^{-1}A^2+\beta^{-2}\Delta_0^2)^2-\frac{\alpha^2\omega_c^2}{(1+\alpha)^2}}, \tag{27}$$

and on the interval $|\omega|\in[\omega_e,\omega_+]$ as Eq. (24).

If $\Delta_0\neq 0$ and is such that $\Delta_0^2>\beta\alpha A^2$, then there is MI if $|\omega|\leqslant\omega_e$ and the corresponding MI gain is Eq. (26). There is also MI if $|\omega|\in[\omega_-,\omega_+]$, and the corresponding MI gain is given by Eq. (24). Note that there is a gap in the spectrum between ω_e and ω_- in which there is no MI.

B. Normal dispersion $\beta<0$, $\sigma_j=0$

If $\Delta_0^2\leqslant 2|\beta|(1-\alpha)A^2$, then there is no MI [26]. There is MI only if $\Delta_0^2>2|\beta|(1-\alpha)A^2$.

More exactly, If $2|\beta|(1-\alpha)A^2<\Delta_0^2\leqslant 2|\beta|(1+\alpha)A^2$, then there is MI if $\omega<\omega_-$. The corresponding MI gain is

$$G(\omega)=2|\beta||\omega|\sqrt{2\beta^{-1}A^2-\beta^{-2}\Delta_0^2-\omega^2-J_0(\omega)} \tag{28}$$

where J_0 is defined by Eq. (25).

If $\Delta_0^2>2|\beta|(1+\alpha)A^2$, then there is MI if $\omega\in[\omega_+,\omega_-]$. The corresponding MI gain is given by Eq. (28).

IV. THE SYSTEM FOR MEAN FIELDS

We will use for the decoupling of the mean values the Furutzu-Novikov formula [28],

$$\langle S_j(z)X\rangle=\langle S_j\rangle\langle X\rangle+\int_0^z\gamma_j(z-z')\left\langle\frac{\delta X(z)}{\delta S_j(z')}\right\rangle dz',$$

where γ_j is the autocorrelation function of the process $S_j-\langle S_j\rangle$, which is assumed to be white noise so that $\gamma_j(z)=2\sigma_j^2\delta(z)$. $\delta X/\delta S_j$ stands for the variational derivative of X with respect to S_j. For instance, Eq. (17) implies that $\delta c(z)/\delta S_1(z)=-i\omega e(z)$, so that $\langle S_1(z)c\rangle=-i\omega\sigma_1^2\langle e\rangle$. Then the system of equations for the row vector of mean fields $\langle\vec{q}\rangle=(\langle c\rangle,\langle d\rangle,\langle e\rangle,\langle f\rangle)^T$ is

$$\frac{d\langle\vec{q}\rangle}{dz}=(Q-\sigma^2\omega^2\mathrm{Id}_4)\langle\vec{q}\rangle, \tag{29}$$

where Id_4 is the 4×4 identity matrix, $\sigma^2:=\sigma_1^2+\sigma_2^2+\sigma_3^2$, and Q is given by Eq. (22). The gain for mean fields is equal to twice the maximal value of the real parts of the eigenvalue of the matrix $Q-\sigma^2\omega^2\mathrm{Id}_4$. The eigenvalue analysis shows that the effect of the PMD fluctuations is to shift all eigenvalues by the term $-\sigma^2\omega^2$ with respect to the homogeneous configuration $\sigma=0$. It thus appears that the effects of randomness, as far as the mean fields are concerned, are the following. (i) The MI gain is reduced. (ii) The MI spectrum is narrower. Nevertheless, as we shall see in the next section, these results are not relevant from the point of view of modulational instability growth, since the first moments of the fields do not capture the exponential growth of the modulus of the fields because of the presence of fast random phases.

V. SYSTEM FOR MEAN INTENSITIES

It should be noted that the first-order moments do not lead to a prediction of resonant phenomena. For a search of resonant processes, it is necessary to investigate the behavior of the second moments. The problem at hand is indeed analogous to the harmonic oscillator with a randomly perturbed frequency,

$$v_{zz}+\omega_0^2[1+\xi(z)]v=0, \tag{30}$$

where $\xi(z)$ is the Gaussian random process. The equations for the first moments obey a trivial dynamics. Indeed, the stochastic parametric resonance is only observed from the second-order moments equations [28].

It can be easily shown that a study of the spatial growth rates of the first moments of the modulations does not correctly capture the growth rate of the intensity of the modulation, when it is averaged over the ensemble of fibers that generate the random processes $S_j(z)$. In fact, the spatial growth rates of the average values of the components of the modulations are reduced owing to random phase factors of the kind $\exp\pm i[\omega\int_0^z S_j(z')dz']$ that multiply the coefficients c, d, e, and f; as a result, the expectation values of these coefficients decay exponentially along z. Therefore, it is necessary to consider the growth of the second-order moments $r_1:=(\langle|c|^2\rangle,\langle|d|^2\rangle,\langle|e|^2\rangle,\langle|f|^2\rangle)$, which are directly related to the intensity of the modulation. Unfortunately, the vector r_1 does not satisfy a closed-form differential equation, and it is necessary to complete the vector r_1 with other second-order moments to get a well-posed problem.

If $\Delta_0=0$, denoting

$$r_2:=\mathrm{Re}(\langle c^*d\rangle,\langle c^*e\rangle,\langle c^*f\rangle,\langle d^*e\rangle,\langle d^*f\rangle,\langle e^*f\rangle),$$

the ten-dimensional row vector $r:=(r_1,r_2)^T$ satisfies the closed-form differential equation

$$\frac{dr}{dz}=Mr, \tag{31}$$

where M is a 10×10 matrix whose explicit form is given in Appendix A. Instability occurs whenever an eigenvalue of M has a positive real part, and the MI gain, which corresponds to an exponential growth of $\langle|c|^2\rangle$, $\langle|d|^2\rangle$, $\langle|e|^2\rangle$, or $\langle|f|^2\rangle$, is twice as large as the value of the real parts of the eigenvalues of M.

If $\Delta_0\neq 0$, denoting

$$r_3:=\mathrm{Im}(\langle c^*d\rangle,\langle c^*e\rangle,\langle c^*f\rangle,\langle d^*e\rangle,\langle d^*f\rangle,\langle e^*f\rangle),$$

the 16-dimensional row vector $\tilde{r}:=(r_1,r_2,r_3)^T$ satisfies the closed-form differential equation

$$\frac{d\tilde{r}}{dz}=\tilde{M}\tilde{r},\quad \tilde{M}=\begin{pmatrix} M & N\\ P & R\end{pmatrix}, \tag{32}$$

where N, P, and R are, respectively, 10×6, 6×10, and 6×6 matrices whose explicit forms are given in Appendix A.

Henceforth, we simplify the algebra by considering the case $B=A$. The study of MI consists in finding the largest value of the real parts of the 10 eigenvalues of the matrix M. Although all coefficients of the matrices are explicitly known, such a problem is intricate and it is difficult to write down the MI gain in a closed form. Nevertheless, in the limiting cases of either small PMD fluctuations $|\beta|^{-1}\sigma_j^2\ll 1$ or large fluctuations $|\beta|^{-1}\sigma_j^2\gg 1$, respectively, we will be able to obtain explicit expansions for the MI gain. Furthermore, by using the MAPLE code [29], we can solve the eigenvalue problem with high accuracy, and plot the MI gain as a function of the frequency ω for any given set of values for A, Δ_0, σ_j, β, and α.

In view of the particular form of the matrix $\tilde{M}$, results corresponding to any power A^2 can be deduced from results of an equivalent problem in which $A=1$ through the transformation

$$\tilde{M}_{ij}(\varepsilon A,\beta,\varepsilon\Delta_0,\sigma_j^2,\alpha,\varepsilon\omega)=\varepsilon^2\tilde{M}_{ij}(A,\beta,\Delta_0,\sigma_j^2,\alpha,\omega)$$

for all $i,j=1,\ldots,16$. Consequently, if one finds that there is MI for some configuration $(A_0,\beta,\Delta_0,\sigma_j^2,\alpha)$ for $\omega\in[\omega_0,\omega_1]$ with gain $G_0(\omega)$, then we can claim that there is MI for the configuration $(\varepsilon A_0,\beta,\varepsilon\Delta_0,\sigma_j^2,\alpha)$ for $\omega\in[\varepsilon\omega_0,\varepsilon\omega_1]$ with gain $\varepsilon^2G_0(\varepsilon^{-1}\omega)$ for any $\varepsilon>0$. This scaling property thus allows straightforward extrapolations that are useful for theoretical analysis as well as for experimental investigations.

VI. ANOMALOUS DISPERSION

A. Expansion of the MI gain for zero mean GVM

We consider in this section the particular case $\Delta_0=0$. In the homogeneous configuration $\sigma_j=0$, $j=1,2,3$, we get back the results of Sec. III A showing that the frequencies below the critical value ω_c are unstable and that the MI gain is Eq. (23). If the birefringence parameters of the fiber are random, then we find that the MI region is increased so that all frequencies are unstable as soon as $\sigma_j^2>0$ for $j=2$ or 3, while the MI gain peak is reduced. The MI peak is equal to $2(1+\alpha)A^2$ when $\sigma_j=0$, and we shall see that it decays to $2A^2$ as σ_j, $j=2$ or 3, increases. We can give the first terms of the asymptotic expansion of the MI gain in the limit of small noise $\beta^{-1}\sigma_j^2\ll 1$. For $|\omega|<\omega_c$, the MI gain is reduced,

$$G(\omega)=2\beta|\omega|\sqrt{\omega_c^2-\omega^2}-2\omega^2(\sigma_2^2+\sigma_3^2). \tag{33}$$

For $|\omega|>\omega_c$, the MI gain is positive while it is zero for $\sigma_j=0$,

$$G(\omega)=G_2(\omega)\sigma_2^2+G_3(\omega)\sigma_3^2, \tag{34}$$

where

$$G_2(\omega)=4\frac{(1-\alpha^2)\beta^{-2}A^4}{K_1(\omega)}+G_3(\omega), \tag{35}$$

$$G_3(\omega)=4\omega^2\frac{K_0K_1(\omega)-K_0^2(\omega)+10\alpha^2\beta^{-2}A^4}{3K_0K_1(\omega)+5K_0^2(\omega)-20\alpha^2\beta^{-2}A^4}, \tag{36}$$

$$K_0(\omega)=\omega^2-2\beta^{-1}A^2, \tag{37}$$

$$K_1(\omega)=\sqrt{\omega^4-4\beta^{-1}A^2\omega^2+4\beta^{-2}(1-\alpha^2)A^4}. \tag{38}$$

Note that σ_1 does not appear in this expression, which means that fluctuations of S_1 do not induce any modification of the MI gain spectrum. If $\alpha=1$, then G_2 and G_3 are equal, which shows that the influences of S_2 and S_3 are equivalent. If $\alpha<1$, then S_2 involves a stronger effect characterized by the first term on the right-hand side of Eq. (35).

We have checked the accuracy of the expansions derived above compared with the full intricate theoretical expressions. We have compared the exact MI gain (obtained with MAPLE) with the expansion (34), which is only valid up to terms of order 2 with respect to $\beta^{-1}\sigma_j^2$. We have seen that, for relatively small values of σ_j (less than 0.3), the expansion (34) is a very good approximation of the real gain.

B. Analysis of the general case $\Delta_0\neq 0$

If $\Delta_0^2<\beta\alpha A^2$ and $\sigma_j=0$, then the MI gain is found to be in a band of frequencies below the critical value ω_+. By taking into account the fluctuations $\sigma_j>0$, $j=1,2,3$, one finds that there is MI for all frequencies.

If $\Delta_0^2\geqslant\beta\alpha A^2$ and $\sigma_j=0$, the MI gain consists of a first peak corresponding to low frequencies and a second peak that lies close to $\beta^{-1}|\Delta_0|$, more precisely between ω_- and ω_+. When taking into account PMD fluctuations, the second peak is strongly reduced and finally it disappears for large σ_j. However, new peaks may appear at low frequencies in the case of large fluctuations of S_j. The analysis can be made clearer by considering separately the influences of the different types of variations of the birefringence parameters S_j, $j=1,2,3$.

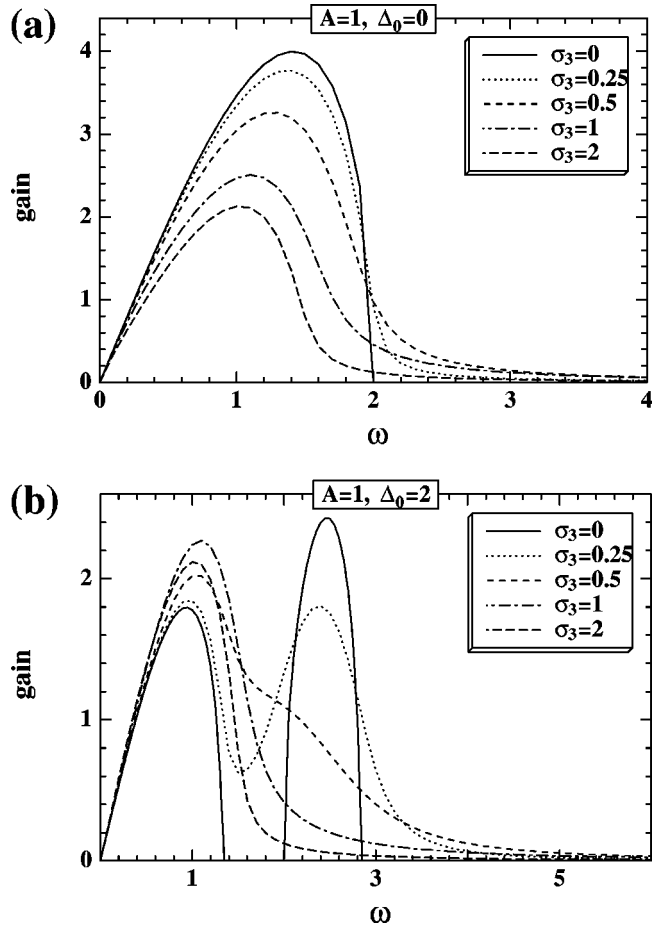

FIG. 1. MI gain vs frequency for an anomalous dispersion $\beta=1$, $\alpha=1$ and different GVM means Δ_0 and deviations σ_3.

C. Fluctuations of S_3

Assume in this section that $\sigma_1=\sigma_2=0$. Figure 1 plots the MI gain spectrum versus increasing values of the standard deviation σ_3 for different GVM means Δ_0. It shows the conversion of the gain spectrum from the deterministic configuration that strongly depends on Δ_0 to an asymptotic form that seems to be independent of Δ_0. This observation can be proved rigorously. Applying the technique developed in Appendix B, we get that the MI spectrum in the asymptotic configuration $\beta^{-1}\sigma_3^2 \gg 1$ does not depend on Δ_0. Independent of Δ_0, the gain for large $\beta^{-1}\sigma_3^2$ is equal to

$$G(\omega)=2\beta|\omega|\sqrt{2\beta^{-1}A^2-\omega^2} \tag{39}$$

if $|\omega|<\sqrt{2}\beta^{-1/2}|A|$ and 0 otherwise. This result is not surprising. The stability conditions for the system (17)–(20) when $S_1=S_2=0$ are equivalent to requiring the stability of the auxiliary system,

$$\tilde{c}_z-\beta\omega^2\tilde{d}=0,$$

$$\tilde{e}_z-\beta\omega^2\tilde{f}=0,$$

$$-\tilde{d}_z-\beta\omega^2\tilde{c}+2A[A\tilde{c}+\alpha(z)^*B\tilde{e}]=0,$$

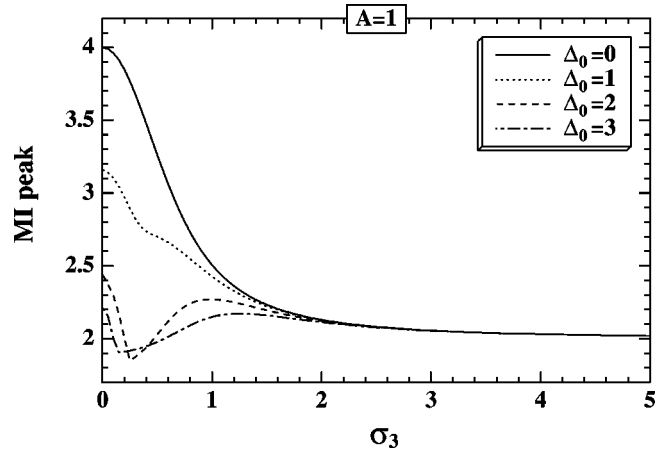

FIG. 2. MI peak (a) vs PMD deviations σ_3 for an anomalous dispersion $\beta=1$, $\alpha=1$, and different GVM means Δ_0.

$$-\tilde{f}_z-\beta\omega^2\tilde{e}+2B[B\tilde{e}+\alpha(z)A\tilde{c}]=0,$$

where $\tilde{c}=c\exp i\phi(z)$, $\tilde{d}=d\exp i\phi(z)$, $\tilde{e}=e\exp -i\phi(z)$, $\tilde{f}=f\exp -i\phi(z)$, and $\phi(z)=\omega\int_0^z S_3(y)dy$, which obeys the statistical distribution of a Brownian motion. The study of MI of electromagnetic waves with a random birefringence $S_3(z)$ is therefore equivalent to the study of MI of electromagnetic waves with a random cross-phase modulation coefficient $\alpha(z):=\alpha\exp 2i\phi(z)$. For very large σ_3, the coupling coefficient has a very fast random phase which makes it average to 0. The limit system $\beta^{-1}\sigma_3^2\gg 1$ corresponds to a decoupled Manakov system with $\alpha=0$. From the results of Sec. III A, Eq. (39) can be interpreted as the gain of the decoupled Manakov system with $\alpha\equiv 0$, $S_3\equiv 0$.

The MI peak versus the amplitude of the noise is plotted in Fig. 2. It shows rather chaotic behaviors depending strongly on Δ_0 for small values of σ_3, but all curves finally converge to $2A^2$, which is the MI peak corresponding to Eq. (39). The mechanism behind these irregularities is made clearer by considering the variations of the optimal frequency. It may happen that the optimal frequency jumps from one value to another, and this is due to the fact that the high-frequency peak is canceled by the PMD fluctuations, while the low-frequency peak converges to Eq. (39). Nevertheless, independent of the initial GVM mean Δ_0, the optimal frequency converges to $\beta^{-1/2}|A|$ as σ_3 increases, which is the optimal frequency corresponding to Eq. (39).

D. Fluctuations of S_2

Figure 3 plots the MI gain spectrum versus increasing values of the standard deviation σ_2. This confirms the asymptotic result obtained by applying Appendix B, which claims that, in the limit $\beta^{-1}\sigma_2^2\gg 1$, independent of Δ_0, the MI gain spectrum consists of two parts:

$$G(\omega)=2\sqrt{1-\alpha^2}A^2 f\left(\frac{\sigma_2\omega}{\sqrt{2}\sqrt[4]{1-\alpha^2}A}\right)$$
$$+2\sqrt{A^4(\alpha^2-1)+2A^2\beta\omega^2-\beta^2\omega^4}, \tag{40}$$

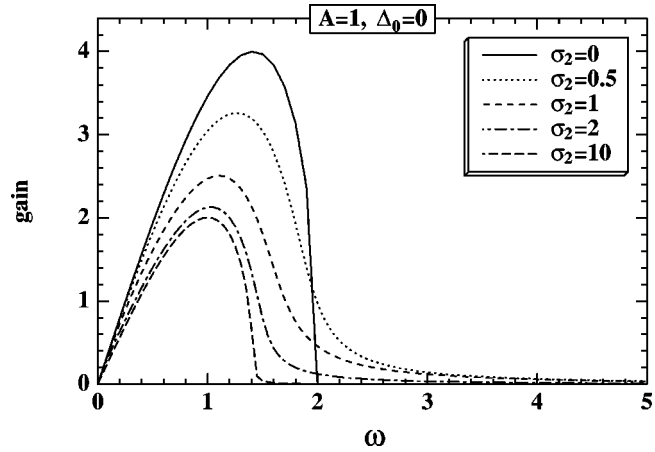

FIG. 3. MI gain vs frequency for an anomalous dispersion $\beta=1$, $\alpha=\frac{2}{3}$, GVM mean $\Delta_0=0$, and fluctuations of S_2.

where

$$f(w)=\frac{1}{3}\frac{(4w^2-\sqrt[3]{54w^2+64w^6+6\sqrt{3}w^2\sqrt{27+64w^4}})^2}{\sqrt[3]{54w^2+64w^6+6\sqrt{3}w^2\sqrt{27+64w^4}}}. \tag{41}$$

This shows that there exist two bands of unstable frequencies. The first one consists of low frequencies whose optimum is obtained at $\omega_{\mathrm{opt},1}=(\sqrt{1+\alpha}A)/2\sigma_2$ and its value is $G_{\mathrm{opt},1}=(1-\alpha^2)A^2$. It is independent of β, it vanishes if $\alpha=1$, and it is maximal for $\alpha=0$. The second band of the MI gain spectrum lies at high frequencies. It vanishes if $\alpha=0$ and it is maximal for $\alpha=1$. Its optimum is obtained at $\omega_{\mathrm{opt},2}=\beta^{-1/2}A$ and its value is $G_{\mathrm{opt},2}=2\alpha A^2$, which is larger (smaller) than $G_{\mathrm{opt},1}$ if $\alpha\geqslant\frac{1}{2}$ ($\alpha\leqslant\frac{1}{2}$). Note that, when $\alpha=1$, the MI gains induced by large fluctuations of S_2 and S_3 are the same, but they are very different when $\alpha<1$.

E. Fluctuations of S_1

Applying Appendix B establishes that in the limit $\beta^{-1}\sigma_1^2\gg1$, the MI gain becomes independent of Δ_0. If $\Delta_0=0$, there is no action of S_1. If $\Delta_0\neq0$, large fluctuations of S_1 impose the MI gain spectrum to adopt the shape of the case $\Delta_0=0$. Accordingly, the MI gain spectrum for $\beta^{-1}\sigma_1^2\gg1$ is given by

$$G(\omega)=2\beta|\omega|\sqrt{\omega_c^2-\omega^2}. \tag{42}$$

Fluctuations of S_1 involve an enhancement of the MI peak and a qualitative change of the unstable bandwidth. They make the high-frequency peak disappear while the low-frequency peak widens.

VII. NORMAL DISPERSION

A. Expansion of the MI gain for zero mean GVM

If the PMD is identically zero (i.e., $\Delta_0=0$, $\sigma_j=0$), then there is no MI as shown in Sec. III B. If the birefringence parameters of the fiber randomly fluctuate and the GVM has zero mean $\Delta_0=0$, $\sigma_j^2>0$, then there is MI and all frequencies are unstable. As in the case $\beta>0$, the closed-form expression of the MI gain is too complicated to be written down explicitly. Nevertheless, we can give the first terms of the asymptotic expansion of the MI gain for small PMD fluctuations $|\beta|^{-1}\sigma_j^2\ll1$. We found that for any $|\omega|>0$, the MI gain is positive and it is given by Eq. (34). For instance, if $\alpha=1$, $\beta=-1$, and $\sigma_1=\sigma_2=0$, then the MI gain spectrum is maximal for $\omega_{\mathrm{opt}}=\sqrt{2}(\sqrt{2}-1)^{1/2}A\simeq0.910A$ and it corresponds to a maximal gain of $G_{\mathrm{opt}}=[4(\sqrt{2}-1)(2\sqrt{2}+1)/(5+3\sqrt{2})]A^2\sigma_3^2\simeq0.686A^2\sigma_3^2$. If $\alpha=2/3$, $\omega_{\mathrm{opt}}\simeq1.274A$ and $G_{\mathrm{opt}}\simeq0.245A^2\sigma_3^2$.

B. Analysis of the general case $\Delta_0\neq0$

As discussed in Sec. III B, if $\sigma_j=0$, there is MI for frequencies lying inside a band around $|\beta|^{-1}|\Delta_0|$, more exactly between ω_- and ω_+. When one increases the PMD fluctuations, this peak disappears, but all frequencies are made unstable. We shall analyze the effects of the different types of fluctuations S_j separately.

C. Fluctuations of S_3

Let us first study the effects of fluctuations of S_3 and consider $\sigma_1=\sigma_2=0$. Figure 4 plots the MI gain spectrum for different values of the GVM mean Δ_0 and deviations σ_3 and for $\alpha=1$, $\beta=-1$. In the asymptotic framework $|\beta|^{-1}\sigma_3^2\gg1$, the MI gain is close to 0 up to a term of order σ_3^{-2} for all frequencies. More exactly, for any frequency not too small $\omega>|A|\sigma_3^{-1}$, we have when $|\beta|^{-1}\sigma_3^2\gg1$

$$G(\omega)=\frac{|\beta|\alpha^2A^4}{2A^2-\beta\omega^2}\sigma_3^{-2}. \tag{43}$$

This result is consistent with a comparison with the decoupled Manakov system, which is valid for large fluctuations $|\beta|^{-1}\sigma_3^2\gg1$. Indeed, the decoupled Manakov system for a normal dispersion $\beta<0$ with $\alpha\equiv0$ and $S_3\equiv0$ is not affected by MI. That is why one finds that the MI gain goes to 0 as σ_3 goes to infinity.

The MI peak versus the amplitude of the noise is plotted in Fig. 5. For $\Delta_0=0$, and more generally for small values of Δ_0, it appears that the MI peak first grows with σ_3 and reaches a maximum for some σ_{30} that depends on Δ_0 and α, but not on the power A^2. For $\alpha=1$, $\beta=-1$, and $\Delta_0=0$, one finds that $\sigma_{30}\simeq0.85$. The corresponding optimal frequency is close to $0.91|A|$. For deviations larger than σ_{30}, the gain and the optimal frequency decay to 0.

If $\Delta_0\neq0$, then the MI peak is also nonzero in the absence of fluctuations, given by $G_{\mathrm{opt}}\simeq2\alpha A^2$ for $\Delta_0^2\gg|\beta|A^2$, and corresponds to an optimal frequency $\omega_{\mathrm{opt}}^2\simeq\beta^{-2}\Delta_0^2+2A^2\beta^{-1}$. Stronger fluctuations lead to a decrease of the peak gain and of the optimal frequency to 0: for large σ_3, the MI gain behaves like in Eq. (43).

D. Fluctuations of S_2

Figure 6 plots the MI gain spectrum for increasing values of σ_2. In the limit $|\beta|^{-1}\sigma_2^2\gg1$, the MI gain becomes independent of β and is given by

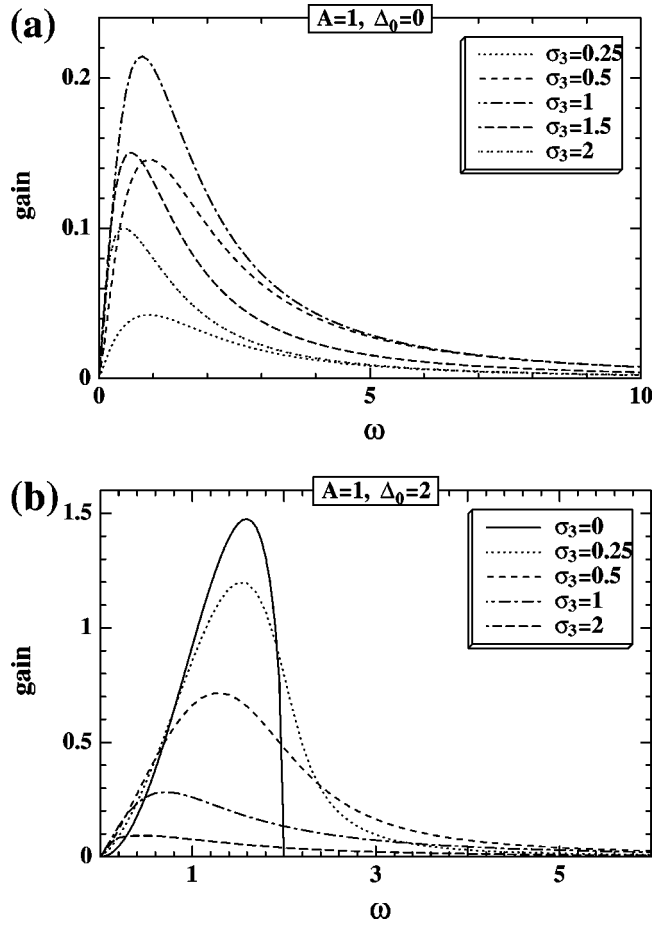

FIG. 4. MI gain vs frequency for a normal dispersion $\beta=-1$, $\alpha=1$, and different GVM means Δ_0 and deviations σ_3. Remember the MI gain is zero for all frequencies in the absence of PMD. $\Delta_0=0$, $\sigma_3=0$.

$$G(\omega)=2\sqrt{1-\alpha^2}A^2 f\left(\frac{\sigma_2\omega}{\sqrt{2}\sqrt[4]{1-\alpha^2}A}\right), \tag{44}$$

where f is defined by Eq. (41). This shows that there exists a band of unstable low frequencies. The optimal MI gain is obtained at $\omega_{\rm opt}=(\sqrt{1-\alpha^2}A)/2\sigma_2$ and its value is $G_{\rm opt}=(1-\alpha^2)A^2$. Note that the MI peak may become higher than in the homogeneous case, and that in the case $\alpha=1$, the MI gain spectrum completely vanishes.

E. Fluctuations of S_1

In the limit $|\beta|^{-1}\sigma_1^2\gg 1$, the MI gain becomes independent of Δ_0. When $\Delta_0=0$, there is no action of S_1, and when $\Delta_0\neq 0$, large fluctuations of S_1 impose the MI gain spectrum to adopt the shape of the case $\Delta_0=0$. Thus the peak that exists in the homogeneous medium in the case $\Delta_0\neq 0$ vanishes.

VIII. UNIFORM FLUCTUATIONS OF PMD

We can also perform an asymptotic study in the framework in which all σ_j are equal. We may think that this is the case for most experimental configurations. In the case of small fluctuations $\sigma_j\equiv\sigma\ll 1$, the expansions derived in the above sections are valid. Let us discuss the case $\Delta_0=0$. In the anomalous regime, the MI gain spectrum is given by Eq. (33) for $|\omega|<\omega_c$ and Eq. (34) for $|\omega|>\omega_c$. One can thus observe that fluctuations of birefringence parameters involve a broadening of the MI spectrum and a reduction of the MI peak. In the normal regime, the MI gain spectrum is given by Eq. (34) for $|\omega|>\omega_c$, which shows that all frequencies are made unstable.

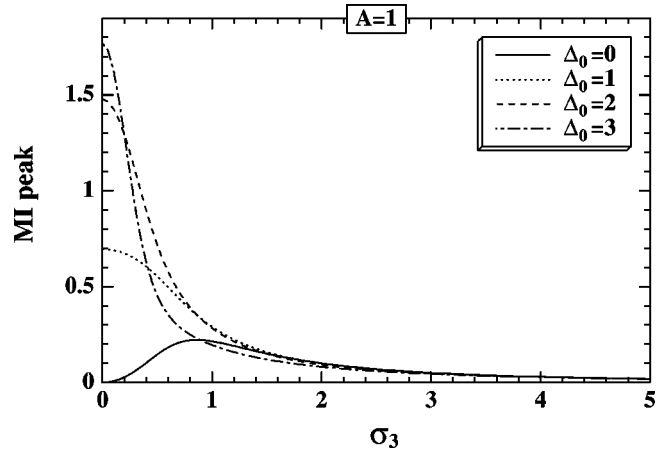

FIG. 5. MI peak vs PMD deviations σ_3 for a normal dispersion $\beta=-1$, $\alpha=1$, and different GVM means Δ_0.

In the case of large fluctuations $\sigma_j\equiv\sigma\gg 1$, we found that the values of β and Δ_0 play no role, while the value of α has only a small quantitative influence. The asymptotic MI gain does not depend on S_1, but only on S_2 and S_3. Qualitatively, one can say that for large fluctuations of the birefringence parameters $|\beta|^{-1}\sigma^2\gg 1$, the MI spectrum is progressively concentrated at low frequencies, and that there is a MI peak (of order A^2) at some low optimal frequency [of order $A/(\sqrt{2}\sigma)$]:

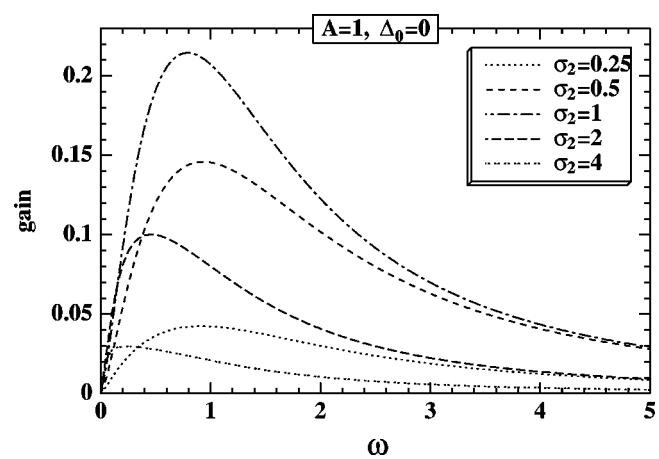

FIG. 6. MI gain vs frequency for a normal dispersion $\beta=-1$, $\alpha=1$, GVM mean $\Delta_0=0$, and different standard deviations of S_2. Remember the MI gain is zero for all frequencies in the absence of PMD. $\Delta_0=0$, $\sigma_j=0$.

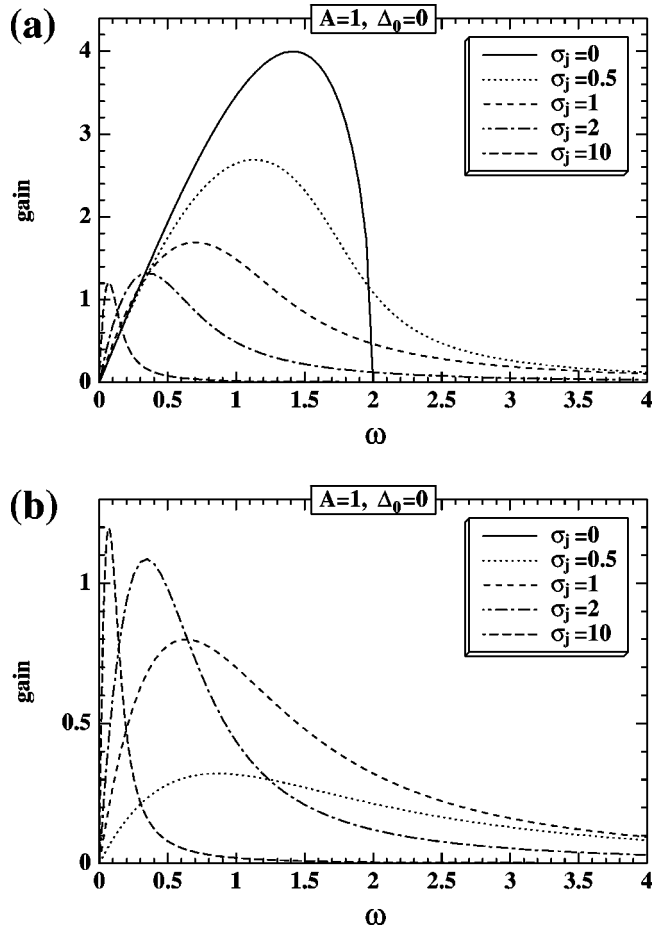

FIG. 7. MI gain vs frequency for an anomalous dispersion $\beta=1$ (a) and normal dispersion $\beta=-1$ (b), GVM mean $\Delta_0=0$, $\alpha=1$, and different standard deviations of S_j. Here we assume $\sigma_1=\sigma_2=\sigma_3$.

$$G(\omega)\simeq 2A^2 f\left(\frac{\sigma\omega}{2A}\right).$$

Figure 7 plots the MI spectra of various configurations for increasing values of the standard deviations $\sigma_1=\sigma_2=\sigma_3$. As can be seen, for large birefringence fluctuations the MI spectrum is concentrated at low frequencies.

IX. NUMERICAL SIMULATIONS OF THE MODULATIONAL INSTABILITY

In this section, we present an example of the comparison of the predictions of the effective system for mean intensities with the direct numerical simulations of the stochastic Manakov system. We performed numerical simulations of the system (3) with a randomly varying birefringence $S_3(z)$. The simulations were done using the split-step Fourier method and the discrete value of the deviation σ_3 is $\sigma_{\rm dis}=\sigma_3/\sqrt{dz}$, where dz is the z step. The initial state is

$$u_1=v_1=\epsilon e^{-i\omega t}+\epsilon e^{i\omega t}, \tag{45}$$

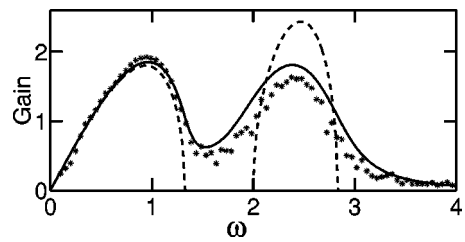

FIG. 8. Gain curve for $\beta=1$, $\Delta_0=2$, $A=1$, and $\sigma_3=0.25$. Stars: numerics; solid curve: linear stability analysis; dashed curve: deterministic MI gain.

with $\epsilon=10^{-4}$. The number of points in the time domain was 256 and the z step was a small fraction of the propagation length ($dz=L/2000$).

The results of the numerical simulations in the *anomalous* dispersion regime are presented in Fig. 8. Theory (solid curve) predicts a decrease in the gain and an extension of the MI gain spectral width with respect to the unperturbed case $\sigma_3=0$ (dashed curve). As can be seen, good agreement was obtained between theoretical predictions and numerical simulations (stars).

The results for the *normal* dispersion regime are shown in Fig. 9. Here the theory predicts an extension of the spectral width of the MI gain, and instability for all modulation frequencies. These predictions are confirmed by numerical simulations. The gain values agree well with theoretical estimates. With decreasing Δ_0, we observed a reduction to zero of the spectral width of the deterministic MI gain and the growth of the spectral width of the gain due to the random modulations of fiber. In the limit case of $\Delta_0=0$, the gain originates entirely from the randomness of the birefringent medium.

An evolution of the spectral intensity of the self-modulated quasicontinuous wave field along the propagation distance is presented in Fig. 10 for the case of the normal group velocity dispersion. One can see that in the initial stage of evolution, the exponential gain growth is accompanied by some oscillations, whereas the asymptotic value of the MI gain (for $z>10$) is in good agreement with the theoretical prediction (dashed line).

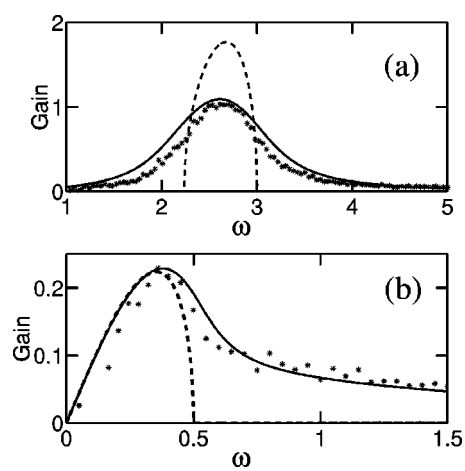

FIG. 9. MI gain curves for $\beta=-1$, $A=1$, and $\sigma_3=0.25$. In the pictures (a) and (b) Δ_0 is equal to 3 and 0.5, respectively.

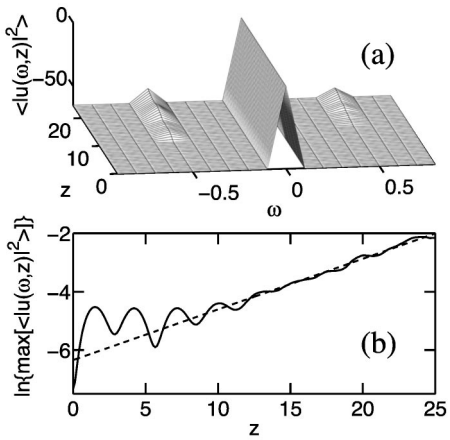

FIG. 10. Evolution of the mean intensity spectrum (in ln scale) along the fiber (a). Optimal gain of the mean intensity spectrum vs the distance propagation z (b). The dashed line corresponds to the estimated growth rate. The averaging has been realized over 200 realizations. The parameters are $\beta=-1$, $A=1$, $\sigma_3=0.25$, and $\Delta_0=0.5$ [as in Fig. 9(b)].

X. CONCLUSION

In conclusion, we investigated the evolution of the MI gain spectrum in optical fibers in the presence of linear random birefringence. We included in the model both a random variation of the absolute value of the birefringence as well as a random coupling between the two fiber axes. Using a linear stability analysis and random process theory, we obtained for the white-noise model of fluctuations of birefringence a system of equations for the second moments. We proved that the MI gain can be obtained as the maximal eigenvalue of a constant effective matrix. On the one hand, we were able to derive analytical expressions for the MI gain in the limit of either small or large standard deviations σ_j of the birefringence noise process. On the other hand, for arbitrary values of σ_j, the spectral domains of MI gain could be easily computed from our analysis by using commonly available software such as MAPLE. We considered both the anomalous and normal dispersion regimes of propagation of continuous beams in fibers. For the anomalous dispersion regime, we predicted an extension of the spectral width of the main gain curve. In other words, we found that in the presence of random birefringence, an intense continuous wave in the anomalous dispersion regime will be unstable with respect to relatively high frequency modulations, which otherwise would not lead to MI in a constant birefringence fiber. On the other hand, in the normal dispersion regime, MI gain is predicted, in principle, for all modulations through phase matching mediated through the random frequency content of the birefringence variations. We have also distinguished between two types of variations of birefringence, depending on whether they involve a reduction or an enhancement of the MI peak. Indeed, as a general conclusion, we obtained that even when the deterministic case is completely stable, birefringence randomness may lead to polarization MI.

In a particular case, we checked the analytical predictions based on the linear stability analysis by means of numerical simulations of the full stochastic system of coupled modified NLS equations. We found good agreement between theoretical predictions and the results of numerical simulations. From the present analysis, we may expect that a similar extension of the MI domain will be observed in a dispersion-managed optical transmission line, where fibers with opposite signs of dispersion are concatenated to combine a low path-average dispersion with a relatively high local dispersion. We plan to investigate this case in future work.

ACKNOWLEDGMENTS

The work of F. Kh. Abdullaev was partially supported by the INTAS (Grant No. 96-0339). This work was also partially sponsored by a contract between the University of Bourgogne and the Centre National d'Etudes des Télécommunications (CNET).

APPENDIX A: EXPLICIT FORMS OF THE MATRICES M AND $\tilde{M}$

We present here the explicit forms of the matrices M and $\tilde{M}$ which appear in Eqs. (31) and (32), respectively:

$$M=-2(\sigma_1^2+\sigma_2^2+\sigma_3^2)\omega^2\mathrm{Id}_{10}+\begin{pmatrix} M_{11} & M_{12} \\ M_{21} & M_{22}\end{pmatrix},$$

where Id_{10} is the 10×10 identity matrix. M_{11} is the 4×4 matrix,

$$M_{11}=2\omega^2\begin{pmatrix} \sigma_3^2 & 0 & \sigma_1^2 & \sigma_2^2 \\ 0 & \sigma_3^2 & \sigma_2^2 & \sigma_1^2 \\ \sigma_1^2 & \sigma_2^2 & \sigma_3^2 & 0 \\ \sigma_2^2 & \sigma_1^2 & 0 & \sigma_3^2\end{pmatrix}.$$

M_{12} is the 4×6 matrix,

$$M_{12}=\begin{pmatrix} 2\beta\omega^2 & 0 & 0 & 0 & 0 & 0 \\ 2A_\omega & 0 & 0 & 2C & 0 & 0 \\ 0 & 0 & 0 & 0 & 0 & 2\beta\omega^2 \\ 0 & 0 & 2C & 0 & 0 & 2B_\omega\end{pmatrix}.$$

M_{21} is the 6×4 matrix,

$$M_{21}=\begin{pmatrix} A_\omega & \beta\omega^2 & 0 & 0 \\ 0 & 0 & 0 & 0 \\ C & 0 & 0 & 0 \\ 0 & 0 & C & 0 \\ 0 & 0 & 0 & 0 \\ 0 & 0 & B_\omega & \beta\omega^2\end{pmatrix}.$$

M_{22} is the 6×6 matrix,

$$M_{22}=\begin{pmatrix} 2\sigma_3^2\omega^2 & C & 0 & 0 & 0 & 2(\sigma_1^2-\sigma_2^2)\omega^2 \\ 0 & 2(\sigma_1^2-\sigma_3^2)\omega^2 & \beta\omega^2 & \beta\omega^2 & -2\sigma_2^2\omega^2 & 0 \\ 0 & B_\omega & 2(\sigma_2^2-\sigma_3^2)\omega^2 & 2\sigma_1^2\omega^2 & \beta\omega^2 & 0 \\ 0 & A_\omega & 2\sigma_1^2\omega^2 & 2(\sigma_2^2-\sigma_3^2)\omega^2 & \beta\omega^2 & 0 \\ C & -2\sigma_2^2\omega^2 & A_\omega & B_\omega & 2(\sigma_1^2-\sigma_3^2)\omega^2 & C \\ 2(\sigma_1^2-\sigma_2^2)\omega^2 & C & 0 & 0 & 0 & 2\sigma_3^2\omega^2 \end{pmatrix}$$

with $B_\omega=2B^2-\beta\omega^2$, $A_\omega=2A^2-\beta\omega^2$, and $C=2\alpha AB$.

$$N=-2\omega\Delta_0\begin{pmatrix} 0&0&0&0&0&0\\ 0&0&0&0&0&0\\ 0&0&0&0&0&0\\ 0&0&0&0&0&0\\ 0&0&0&0&0&0\\ 0&1&0&0&0&0\\ 0&0&1&0&0&0\\ 0&0&0&1&0&0\\ 0&0&0&0&1&0\\ 0&0&0&0&0&0 \end{pmatrix},\quad P=2\omega\Delta_0\begin{pmatrix} 0&0&0&0&0&0&0&0&0&0\\ 0&0&0&0&0&1&0&0&0&0\\ 0&0&0&0&0&0&1&0&0&0\\ 0&0&0&0&0&0&0&1&0&0\\ 0&0&0&0&0&0&0&0&1&0\\ 0&0&0&0&0&0&0&0&0&0 \end{pmatrix},$$

$$R=\begin{pmatrix} 2\sigma_3^2\omega^2 & C & 0 & 0 & 0 & (\sigma_1^2+\sigma_2^2)\omega^2 \\ 0 & -2(\sigma_1^2+\sigma_3^2)\omega^2 & \beta\omega^2 & \beta\omega^2 & 2\sigma_2^2\omega^2 & 0 \\ 0 & B_\omega & -2(\sigma_2^2+\sigma_3^2)\omega^2 & -2\sigma_1^2\omega^2 & \beta\omega^2 & 0 \\ 0 & A_\omega & -2\sigma_1^2\omega^2 & -2(\sigma_2^2+\sigma_3^2)\omega^2 & \beta\omega^2 & 0 \\ -C & 2\sigma_2^2\omega^2 & A_\omega & B_\omega & -2(\sigma_1^2+\sigma_3^2)\omega^2 & C \\ 2(\sigma_1^2+\sigma_2^2)\omega^2 & -C & 0 & 0 & 0 & 2\sigma_3^2\omega^2 \end{pmatrix}.$$

APPENDIX B: EXPANSIONS OF THE EIGENVALUES OF A PERTURBED MATRIX

In this appendix, we attempt to sketch out the derivations of the expansions of the MI gain with respect to the small parameter $|\beta|\sigma^2$. The method is general and can be applied to the following framework. Let us assume that M^0 is a $d\times d$ matrix whose eigenvalues are denoted by λ_l^0, $l=1,\ldots,d$. Let us consider the matrix $M:=M^0+\varepsilon M^1$ and the associated eigenvalues $(\lambda_l^\varepsilon)_{l=1,\ldots,d}$, where ε is a small parameter and M^1 is another $d\times d$ matrix.

Proposition. Let us fix some $l=1,\ldots,d$. If the matrix M^0 [the (i,j)th minor of a matrix M is the matrix obtained by removing the ith row and the jth column of M] satisfies

$$D_0:=\sum_{i=1}^{d}\det(\mathrm{minor}(M^0-\lambda_l^0 I_d)_{ii})\neq 0,$$

then the eigenvalue λ_l^ε can be expanded as powers of ε as

$$\lambda_l^\varepsilon=\lambda_l^0+\varepsilon\lambda_l^1+o(\varepsilon),$$

where the corrective term λ_l^1 is given by

$$\lambda_l^1=\frac{1}{D_0}\sum_{i,j=1}^{d}(-1)^{i+j}\det(\mathrm{minor}(M^0-\lambda_l^0 I_d)_{ij})M_{ij}^1.$$

Proof. We first remember that the ''det'' mapping that associates to every matrix its standard determinant is continuously differentiable and its partial derivatives are given by

$$\frac{\partial\det(M)}{\partial M_{ij}}=(-1)^{i+j}\det(\mathrm{minor}(M)_{ij}).$$

Let us now consider the function

$$\Theta:\begin{cases}\mathbb{R}^2 & \to \quad \mathbb{R}\\ (\lambda,\varepsilon) & \mapsto \quad \det(M^0+\varepsilon M^1-\lambda I_d).\end{cases}$$

This function is continuously differentiable and we have

$$\frac{\partial\Theta}{\partial\lambda}=-\sum_{i=1}^{d}\det(\mathrm{minor}(M^0+\varepsilon M^1-\lambda I_d)_{ii}),$$

$$\frac{\partial\Theta}{\partial\varepsilon}=\sum_{i,j=1}^{d}(-1)^{i+j}\det(\mathrm{minor}(M^0+\varepsilon M^1-\lambda I_d)_{ij})M^1_{ij}.$$

On the one hand, we have $f(\lambda_l^0,0)=0$. On the other hand, we have $[\partial\Theta(\lambda,\varepsilon)/\partial\lambda]|_{(\lambda_0^l,0)}=D_0$, which is nonzero by assumption. Consequently, by applying the implicit function theorem we get that there exists $\varepsilon_0>0$ and a function $\lambda\in\mathcal{C}^1((-\varepsilon_0,\varepsilon_0),\mathbb{R})$ such that

$$\lambda(0)=\lambda_l^0 \text{and } \Theta(\lambda(\varepsilon),\varepsilon)=0 \quad \forall\varepsilon\in(-\varepsilon_0,\varepsilon_0).$$

Moreover this function is continuously differentiable and

$$\frac{\partial\lambda(\varepsilon)}{\partial\varepsilon}=-\frac{\frac{\partial\Theta}{\partial\varepsilon}(\lambda(\varepsilon),\varepsilon)}{\frac{\partial\Theta}{\partial\lambda}(\lambda(\varepsilon),\varepsilon)}.$$

Consequently, applying Taylor's formula,

$$\lambda(\varepsilon)=\lambda(0)+\varepsilon\left.\frac{\partial\lambda(\varepsilon)}{\partial\varepsilon}\right|_{\varepsilon=0}+o(\varepsilon)$$

$$=\lambda_0^l-\frac{\frac{\partial\Theta}{\partial\varepsilon}(\lambda_0^l,0)}{\frac{\partial\Theta}{\partial\lambda}(\lambda_0^l,0)}\varepsilon+o(\varepsilon),$$

which completes the proof of the proposition.

[1] G. B. Whitham, J. Fluid Mech. **27**, 399 (1967).
[2] T. B. Benjamin and J. E. Feir, J. Fluid Mech. **27**, 417 (1967).
[3] V. I. Bespalov and V. I. Talanov, Pisma Zh. Éksp. Teor. Fiz.**3**, 471 (1966) [JETP Lett. **3**, 307 (1966)].
[4] L. A. Ostrowski, Zh. Éksp. Teor. Fiz. **51**, 1189 (1966) [Sov. Phys. JETP **24**, 797 (1967)].
[5] G. P. Agrawal, *Nonlinear Fiber Optics*, 2nd ed. (Academic, New York, 1995).
[6] F. Matera, A. Mecozzi, M. Romagnoli, and M. Settembre, Opt. Lett. **18**, 1499 (1993).
[7] F. Kh. Abdullaev, Pisma Zh. Tekh. Fiz. **20**, 25 (1994) [Tech. Phys. Lett. **20**, 636 (1994)].
[8] N. J. Smith and N. J. Doran, Opt. Lett. **21**, 570 (1996).
[9] F. Kh. Abdullaev, S. A. Darmanyan, S. Bishoff, and M. P. Sørensen, J. Opt. Soc. Am. B **14**, 27 (1997).
[10] F. Kh. Abdullaev, S. A. Darmanyan, A. Kobyakov, and F. Lederer, Phys. Lett. A **220**, 271 (1996).
[11] M. Karlsson, J. Opt. Soc. Am. B **15**, 2269 (1998).
[12] S. Trillo and S. Wabnitz, J. Opt. Soc. Am. B **6**, 238 (1989).
[13] S. Wabnitz, Phys. Rev. A **38**, 2018 (1988).
[14] S. C. Rashleigh and R. Ulrich, Opt. Lett. **3**, 60 (1978).
[15] C. R. Menyuk, IEEE J. Quantum Electron. **25**, 2674 (1989).
[16] L. F. Mollenauer, K. Smith, J. P. Gordon, and C. R. Menyuk, Opt. Lett. **14**, 1219 (1989).
[17] P. K. Wai, C. R. Menyuk, and H. H. Chen, Opt. Lett. **16**, 1231 (1991).
[18] C. De Angelis, F. Materi, and S. Wabnitz, Opt. Lett. **17**, 850 (1992).
[19] C. R. Menyuk and P. K. A. Wai, J. Opt. Soc. Am. B **11**, 1288 (1994); P. K. A. Wai and C. R. Menyuk, J. Lightwave Technol. **14**, 148 (1996).
[20] T. I. Lakoba and D. J. Kaup, Phys. Rev. E **56**, 6147 (1997).
[21] S. G. Evangelides, L. F. Mollenauer, J. P. Gordon, and N. S. Bergano, J. Lightwave Technol. **10**, 28 (1992).
[22] M. Midrio, J. Opt. Soc. Am. B **17**, 169 (1999).
[23] Y. S. Kivshar and V. V. Konotop, Kvant. Elektron. (Moscow) **17**, 1599 (1990).
[24] N. F. Smyth and A. H. Pincombe, Phys. Rev. E **57**, 7231 (1998).
[25] Y. Chen and H. A. Haus, Opt. Lett. **25**, 290 (2000).
[26] J. E. Rothenberg, Phys. Rev. A **42**, 682 (1990).
[27] P. Drummond, Opt. Commun. **78**, 137 (1990).
[28] V. I. Klyatzkin, *Stochastic Differential Equations and Waves in Random Media* (Nauka, Moscow, 1980).
[29] MAPLE V, Waterloo Maple Software, Ontario, Canada.